Electron and Photon Reconstruction and Identification with the ATLAS Detector

Jovan Mitrevski, *Ludwig-Maximilians-Universität München*
for the ATLAS Collaboration

Introduction

The performance of electron and photon reconstruction plays a critical role in the reach of many analyses, including $H \to \gamma\gamma$, $H \to 4\ell$, SUSY, and exotics searches. For the 8 TeV running of the LHC, a number of improvements were made to the reconstruction algorithms to improve the efficiency for low-p_T electrons and at high pileup conditions.

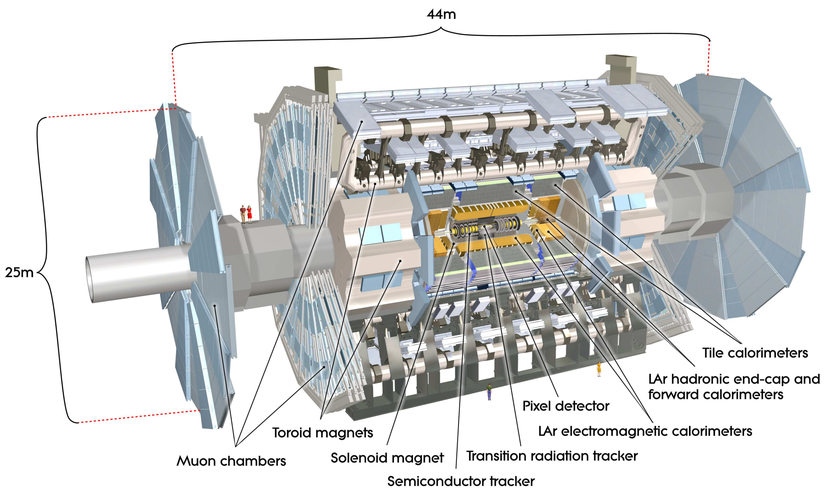

Figure 1: The ATLAS detector.

ATLAS Detector

The ATLAS detector [1], Fig. 1, is a multi-purpose apparatus with a forward-backward symmetric cylindrical geometry and nearly 4π solid angle coverage. It consists of the following detectors, with the inner detector (pixel, SCT, and TRT) being inside a 2 T magnetic field:

i. Pixel and silicon microstrip (SCT) trackers covering $|\eta| < 2.5$.

ii. Transition Radiation Tracker (TRT) covering $|\eta| < 2.0$; also provides discrimination between electrons and charged hadrons based on transition radiation.

iii. Lead/liquid-argon electromagnetic (EM) calorimeter covering $|\eta| < 3.2$; finely segmented in η and ϕ, and with three layers in depth for $|\eta| < 2.5$.

iv. Hadronic calorimeters, followed by the muon system.

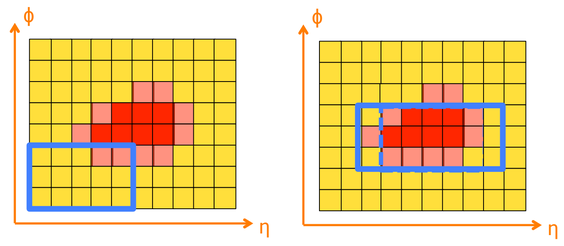

Figure 2: Diagram showing cluster-building.

Electron And Photon Reconstruction

A number of improvements were made to the electron and photon reconstruction for the 8 TeV running. In this section, we outline the standard reconstruction process and indicate the differences. For more information, see Ref. [2].

1. Cluster Building

Standard electron and photon reconstruction starts by building clusters in the EM calorimeter, as show in Fig. 2. The EM calorimeter, using all three layers in depth, is divided into towers of $\Delta\eta \times \Delta\phi = 0.025 \times 0.025$. A sliding-window algorithm [3] with windows of size 3×5 in η - ϕ space is performed, followed by duplicate removal. Based on MC simulations, the efficiency is 95% for electrons with $E_T = 7$ GeV, 99% for those with $E_T = 15$ GeV, and 99.9% for those with $E_T = 45$ GeV.

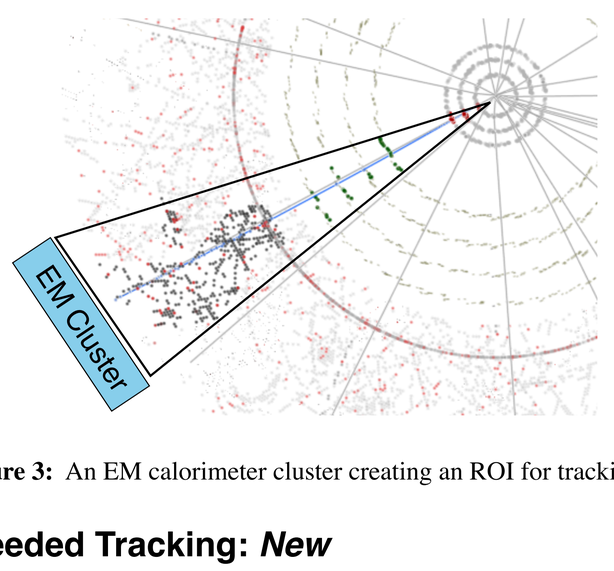

Figure 3: An EM calorimeter cluster creating an ROI for tracking.

2. Seeded Tracking: *New*

Clusters that pass loose shower shape requirements in hadronic leakage and energy distribution in η create Regions of Interests (ROIs), as shown in Fig. 3. Within these ROIs, the tracking is modified as follows.

Pattern recognition: Standard track pattern reconstruction [4] is first performed, using a pion hypothesis. If this fails, a modified pattern reconstruction algorithm, based on a Kalman filter formalism [5], using an electron hypothesis and allowing for up to 30% energy loss at each material surface, is performed.

Additionally, tighter requirements have been made to improve the track purity, especially for TRT stand-alone tracks (TRTSA).

Track fitting: Track candidates are fitted with the global χ^2 fitter [6], using the same particle hypothesis as the pattern recognition initially, but retrying with an electron hypothesis if the original pion hypothesis fails.

Loose matching to the cluster: A set of tracks is considered loosely matched to the cluster if either of the following requirements passes:

i. Tracks are extrapolated to the second layer of the EM calorimeter and are loosely matched in ϕ, and if they have silicon hits, in η.

ii. As i, but the track momenta are rescaled to be as measured in the cluster.

GSF Fitting: Tracks with silicon hits loosely matched to the cluster are refitted with a Gaussian Sum Filter (GSF) fitter [7], a non-linear generalization of the Kalman filter, for improved track parameters, as demonstrated by Fig. 4. These tracks, along with the TRTSA and the small number that fail the refits, are used for track matching and conversion vertex building.

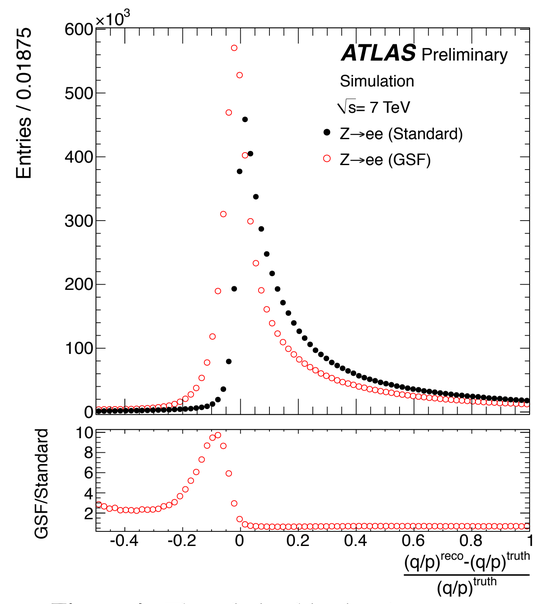

Figure 4: The relative bias in q/p.

3. Track Matching for Electrons

The potentially refitted, loosely-matched tracks are matched to the cluster with slightly tighter requirements in η and ϕ. At least one track must be matched for a cluster to form an electron. If multiple tracks are matched, they are sorted in the following order, with the first being used for the kinematics. Preferred are tracks with hits in the pixel detector, then those with silicon hits but no pixel hits, then TRTSA tracks. Within each category, those that have a better ΔR match in η - ϕ, where the extrapolation is done with the track energy and the cluster energy, are preferred, unless the differences are small, in which case the one with more pixel hits is preferred, giving an extra weight to a hit in the innermost barrel (*b*-layer).

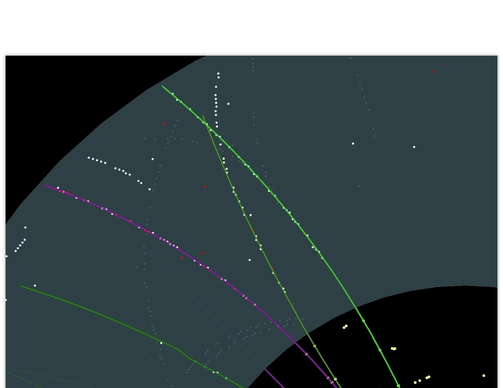

Figure 5: An event display of a double-track conversion

4. Conversion Building for Photons

Conversion-finding is run on the potentially refitted, loosely-matched tracks. Conversions are classified as single-track or double-track. Double-track conversions are created when two tracks form a vertex consistent with coming from a massless particle, as shown in Fig. 5. Single-track conversions are tracks not having hits in the innermost sensitive layers. To increase the purity, the tracks used to build conversions must generally have a high probability to be electron tracks as determined by the TRT, especially to build single-track conversions or if the tracks are TRTSA. The matching between tracks from the conversion vertices and clusters was tightened for the 8 TeV running. Quality and consistency cuts are applied on the conversion vertices for better pileup tolerance.

Because dead pixels can effect conversion building, extra logic has been added to determining what makes a good conversion.

If there are multiple conversion vertices matched, they are sorted in the following order, with the first being used for the kinematics. Double-track conversions with two silicon tracks are preferred over other double-track conversions, followed by single-track conversions. Within each category, the vertex with the smallest conversion radius is preferred.

5. Final Cluster Creation

New, calibrated clusters are created for electrons and photons, of size 3×5 in η - ϕ space for unconverted photons in the barrel calorimeter, 3×7 for electrons and converted photons in the barrel, and 5×5 in the end-caps.

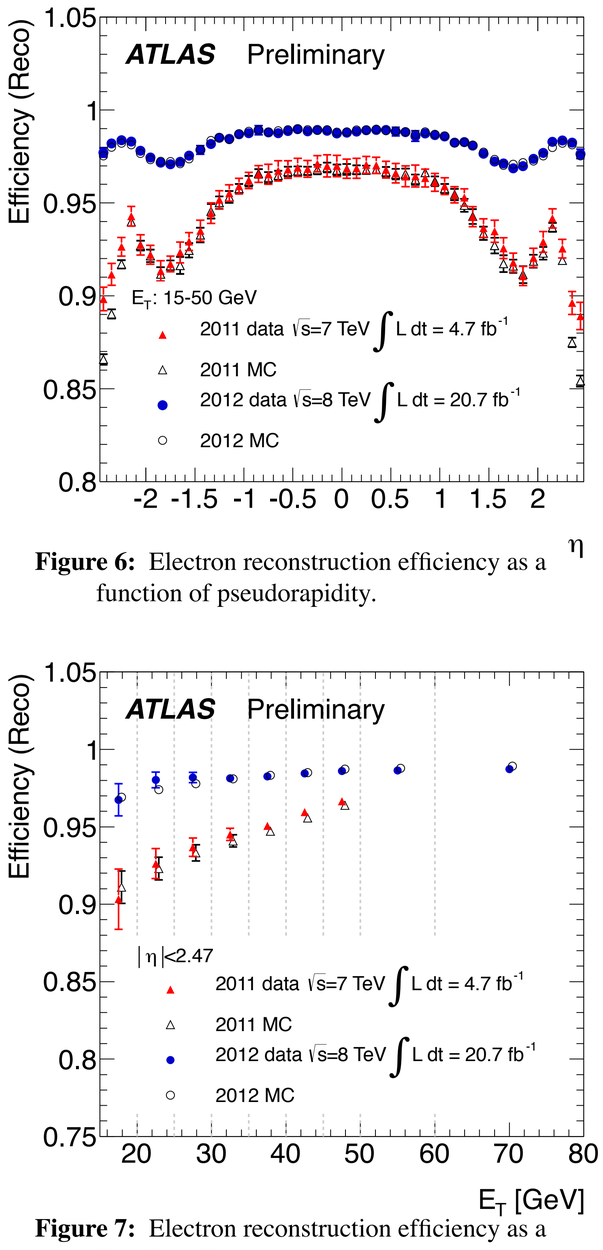

Figure 6: Electron reconstruction efficiency as a function of pseudorapidity.

Figure 7: Electron reconstruction efficiency as a function of transverse energy.

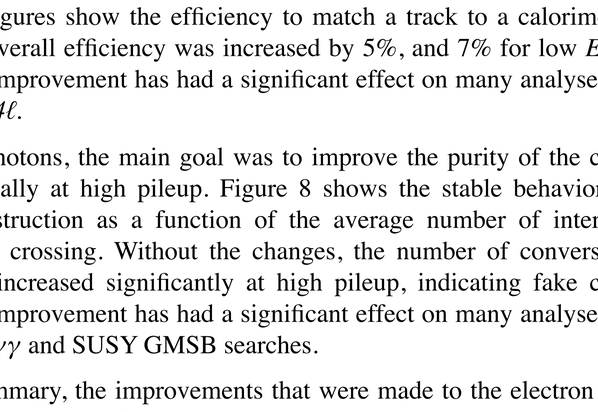

Figure 8: The fraction of photon candidates that are unconverted, single-track conversions, or double-track conversions.

Results and Conclusion

As can be seen in Fig. 6 and Fig. 7, there were significant improvements in the reconstruction efficiency of electrons in the 8 TeV running, especially at low-E_T and at higher pseudorapidity, where the tracks traverse more material and hence are more likely to lose energy due to bremsstrahlung. The figures show the efficiency to match a track to a calorimeter cluster. The overall efficiency was increased by 5%, and 7% for low E_T electrons. This improvement has had a significant effect on many analyses, including $H \to 4\ell$.

For photons, the main goal was to improve the purity of the conversions, especially at high pileup. Figure 8 shows the stable behavior of photon reconstruction as a function of the average number of interactions per bunch crossing. Without the changes, the number of conversions would have increased significantly at high pileup, indicating fake conversions. This improvement has had a significant effect on many analyses, including $H \to \gamma\gamma$ and SUSY GMSB searches.

In summary, the improvements that were made to the electron and photon reconstruction software have been very important in achieving the many physics goals of Run I at ATLAS.

References

[1] ATLAS Collaboration, *The ATLAS Experiment at the CERN Large Hadron Collider*, JINST **3** (2008) S08003.

[2] ATLAS Collaboration, *Electron efficiency measurements with the ATLAS detector using the 2012 LHC proton-proton collision data,* ATLAS-CONF-2014-032, 2014.

[3] W. Lampl et al., *Calorimeter clustering algorithms: description and performance,* ATL-LARG-PUB-2008-002, 2008.

[4] T. Cornelissen et al, *Concepts, design and implementation of the ATLAS new tracking (NEWT),* ATL-SOFT-PUB-2007-007, 2007.

[5] R. Frühwirth, *Application of Kalman filtering to track and vertex fitting*, Nucl. Instrum. Meth. **A262** (1987) 444-450.

[6] T. Cornelissen et al, The global χ^2 track fitter in ATLAS, J. Phys. Conf. Ser. **119** (2008) 032013.

[7] ATLAS Collaboration, *Improved electron reconstruction in ATLAS using the Gaussian Sum Filter-based model for bremsstrahlung*, ATLAS-CONF-2012-047, 2012.